Molecular Pharmacology Fast Forward. Published on February 18, 2005 as DOI: 10.1124/mol.105.010959
Molecular Pharmacology Fast Forward. Published on March 4, 2005 as doi:10.1124/mol.105.010959

Submitted, Molecular Pharmacology

PHENYLGLYCINE AND SULFONAMIDE CORRECTORS OF DEFECTIVE ΔF508- AND G551D-CFTR CHLORIDE CHANNEL GATING

Nicoletta Pedemonte[1,2], N.D. Sonawane[1], Alessandro Taddei[2], Jie Hu[1], Olga Zegarra-Moran[2], Yat Fan Suen[3], Lori I. Robins[3], Christopher W. Dicus[3], Dan Willenbring[3], Michael H. Nantz[3], Mark J. Kurth[3], Luis J.V. Galietta[2] and A.S. Verkman[1]

[1]Departments of Medicine and Physiology, University of California, San Francisco CA 94143-0521, [2]Laboratorio di Genetica Molecolare, Istituto Giannina Gaslini, 16148 Genova, Italy, and [3]Department of Chemistry, University of California, Davis CA.

Molecular Pharmacology Fast Forward. Published on February 18, 2005 as DOI: 10.1124/mol.105.010959
This article has not been copyedited and formatted. The final version may differ from this version.

Running title: Potentiators of ΔF508-CFTR gating

Correspondence:

Alan S. Verkman, M.D., Ph.D.

1246 Health Sciences East Tower, U.C.S.F.

San Francisco, CA 94143-0521, U.S.A.

Phone: (415)-476-8530; Fax: (415)-665-3847

E-mail: verkman@itsa.ucsf.edu; http://www.ucsf.edu/verklab

N. of text pages: 26

N. of figures : 8

N. of tables : 1

N. of references : 34

N. of words in abstract : 242

N. of words in introduction : 604

N. of words in discussion : 721

Abbreviations :

CFTR, cystic fibrosis transmembrane conductance regulator; YFP, yellow fluorescent protein; PG, phenylglycine; SF, sulfonamide ; MDR-1, multidrug resistance protein 1.

Molecular Pharmacology Fast Forward. Published on February 18, 2005 as DOI: 10.1124/mol.105.010959
This article has not been copyedited and formatted. The final version may differ from this version.

ABSTRACT

Mutations in the cystic fibrosis transmembrane conductance regulator (CFTR) chloride channel cause cystic fibrosis. The ΔF508 mutation produces defects in channel gating and cellular processing, whereas the G551D mutation produces primarily a gating defect. To identify correctors of gating, 50,000 diverse small molecules were screened at 2.5 µM (with forskolin, 20 µM) by an iodide uptake assay in epithelial cells co-expressing ΔF508-CFTR and a fluorescent halide indicator (YFP-H148Q/I152L) after ΔF508-CFTR rescue by 24 h culture at 27 ^{o}C. Secondary analysis and testing of >1000 structural analogs yielded two novel classes of correctors of defective ΔF508-CFTR gating (‘potentiators’) with nanomolar potency that were active in human ΔF508 and G551D cells. The most potent compound of the phenylglycine class, 2-[(2-1*H*-indol-3-yl-acetyl)-methylamino]-N-(4-isopropylphenyl)-2-phenylacetamide, reversibly activated ΔF508-CFTR in the presence of forskolin with K_a ~70 nM, and also activated the CFTR gating mutants G551D and G1349D with K_a ~1100 and 40 nM, respectively. The most potent sulfonamide, 6-(ethylphenylsulfamoyl)-4-oxo-1,4-dihydroquinoline-3-carboxylic acid cycloheptylamide, had K_a ~20 nM for activation of ΔF508-CFTR. In cell-attached patch-clamp experiments, PG-01 and SF-01 increased channel open probability >5-fold by reduction of interburst closed time. An interesting property of these compounds was their ability to act in synergy with cAMP agonists. Microsome metabolism studies and rat pharmacokinetic analysis suggested significantly more rapid metabolism of PG-01 than SF-03. Phenylglycine and sulfonamide compounds may be useful for mono-therapy of cystic fibrosis caused by gating mutants and possibly for a subset of ΔF508 subjects with significant ΔF508-CFTR plasma membrane expression.

Molecular Pharmacology Fast Forward. Published on February 18, 2005 as DOI: 10.1124/mol.105.010959
This article has not been copyedited and formatted. The final version may differ from this version.

INTRODUCTION

Cystic Fibrosis (CF), a relatively common hereditary disease in Caucasians, can produce chronic lung infection and deterioration of lung function, pancreatic insufficiency, male infertility, and meconium ileus (Pilewski and Frizzell, 1999). CF is caused by mutations in the cystic fibrosis transmembrane conductance regulator (CFTR) protein, a cAMP-activated Cl^- channel expressed in airway, pancreatic, intestinal, testicular, and other epithelia (Sheppard and Welsh, 1999). ΔF508 is by far the most common CFTR mutation causing CF, being present in ~60 % of CF genes and in ~90 % of CF subjects as at least one allele (Bobadilla et al., 2002). The ΔF508 mutation is thought to produce Cl^- impermeable epithelial cells by aberrant protein folding and consequent defects in cellular processing and channel gating (Dalemans et al., 1991; Denning et al., 1992; Haws et al., 1996; Kopito, 1999). Most ΔF508-CFTR protein is retained at the endoplasmic reticulum and degraded rapidly (Jensen et al., 1995; Ward et al., 1995). Many other CFTR mutations causing CF are targeted to the cell plasma membrane but produce chloride impermeable cells by a primary defect in channel gating. The most common of the CFTR gating mutants is G551D, with a worldwide frequency of 3.1% among CF chromosomes (Hamosh et al., 1992), though persons of Celtic descent have frequencies as high as 8% (Cashman et al., 1995).

Small molecule activators/correctors of mutant CFTRs may provide a strategy for therapy of CF that corrects the underlying defect. Activation of mutant CFTRs avoids potential concerns about treating the wrong cells and/or losing physiological CFTR regulation as might occur with gene therapy or activation of alternative chloride channels. Restoration of cAMP-regulated chloride permeability in epithelial cells expressing ΔF508-CFTR would likely require compound(s) that correct the underlying defects in cellular processing and channel gating, though there may exist a subset of subjects with enough plasma membrane ΔF508-CFTR expression (Penque et al., 2000; Sermet-Gaudelus et al., 2002) to be benefited by a corrector of defective channel gating ('potentiator'). Potentiators may also be useful as mono-therapy for CF caused by gating mutants of CFTR such as G551D.

Various small molecules have been found to have potentiator activity for correction of the ΔF508-CFTR gating defect. Relatively high concentrations of flavones such as genistein (>50 μM) and xanthines such as isobutylmethylxanthine (>1 mM) can restore normal or near normal ΔF508-CFTR channel gating when given with cAMP agonists (Drumm et al., 1991; Haws et al., 1996; Hwang et al., 1997). Flavones at high concentrations also are able to correct defective gating in G551D-CFTR (Illek et al., 1999; Zegarra-Moran et al., 2002). We previously identified a benzothiophene class of ΔF508-CFTR potentiators by high-throughput screening of 100,000 small molecules (Yang et al., 2003). After compound optimization by structure-activity studies, benzothiophenes were identified that rapidly restored near normal ΔF508-CFTR channel gating with K_a ~0.5 μM as measured by short-circuit current analysis. However, activation required high concentrations of cAMP agonists, and the benzothiophenes did not activate CFTR gating mutants such as G551D.

Here, we carried out high-throughput screening to identify novel classes of correctors of defective ΔF508-CFTR channel gating, focusing on compounds with very high potency, potentiator activity in human airway epithelial cells from CF subjects, and activity against other CFTR gating mutants. Two novel classes of potentiators emerged from primary screening and secondary evaluation – phenylglycines and sulfonamides. These compounds were potent in ΔF508-CFTR transfected and natively expressing human cells, active in the presence of relatively low concentrations of cAMP agonists, and active against multiple CFTR gating mutants including G551D. To evaluate their potential utility for drug development, the phenylglycines and sulfonamides were subject to analysis of structure-activity relationships, single-channel electrophysiology, and metabolic stability/*in vivo* pharmacology.

METHODS

Cell lines – Fischer rat thyroid (FRT) epithelial cells stably co-expressing human ΔF508-CFTR and the high-sensitivity halide-sensing green fluorescent analog YFP-H148Q/I152L (Galietta et al., 2001a) were generated as described previously (Yang et al., 2003). FRT cells were cultured on plastic in Coon`s modified F12 medium supplemented with 10% fetal bovine serum, 2 mM L-glutamine, 100 U/ml penicillin, and 100 μg/ml streptomycin. For primary screening, cells were plated using a LabSystems multidrop dispenser into black 96-well microplates (Corning-Costar) at 50,000 cells/well. Screening was done at 18-24 hours after plating. For short-circuit current measurements cells were cultured

Molecular Pharmacology Fast Forward. Published on February 18, 2005 as DOI: 10.1124/mol.105.010959
This article has not been copyedited and formatted. The final version may differ from this version.

on Snapwell permeable supports (Corning-Costar) at 500,000 cells/insert. Human nasal epithelial cells from CF subjects were cultured on Snapwell inserts and allowed to differentiate in a hormone-supplemented medium as described previously (Galietta et al., 1998). Some measurements were done using stably transfected FRT cells expressing YFP-H148Q and wildtype- or G551D-CFTR (Galietta et al., 2001b). Patch-clamp experiments were done on ΔF508-CFTR expressing FRT cells plated on 35 mm Petri dishes.

***Compounds* –** A collection of 50,000 diverse drug-like compounds (>90% with molecular size 250-500 daltons, ChemDiv) was used for initial screening. The compounds were cherry-picked for favorable drug-like properties, maximal chemical diversity, and minimal overlap with 100,000 compounds tested previously. For optimization, >1000 analogs of activators identified in the primary screen were purchased from ChemDiv. Compounds were prepared as 10 mM stock solutions in DMSO. Secondary plates containing one or four compounds per well were prepared for screening (1 mM in DMSO). Compounds for secondary analysis were resynthesized, purified, and confirmed by NMR and liquid chromatography / mass spectrometry.

***Screening procedures* –** Screening was carried out using a Beckman integrated system containing a 3-meter robotic arm, CO_2 incubator containing microplate carousel, plate-washer, liquid handling workstation, bar code reader, delidding station, plate sealer, and two FluoStar fluorescence plate readers (Optima, BMG Lab Technologies), each equipped with dual syringe pumps and HQ500/20X (500 ± 10 nm) excitation and HQ535/30M (535 ± 15 nm) emission filters (Chroma). For assay of ΔF508-CFTR potentiator activity, FRT cells were incubated at 27 ^{o}C (90% humidity, 5% CO_2) to allow rescue of mutant CFTR. After 18-24 hour incubation, plates (40-50 per day) were washed with PBS and cells were incubated with 60 µL of PBS containing forskolin (20 µM) and test compounds (2.5 µM). After 15 min, the 96-well plate was transferred to a plate reader for fluorescence assay. Each well was assayed individually for I^- influx by recording fluorescence continuously (200 ms per point) for 2 s (baseline) and then for 12 s after rapid (<1 s) addition of 165 µL of PBS in which 137 mM Cl^- was replaced by I^-. I^- influx rate was computed by fitting the final 11.5 s of the data to an

Molecular Pharmacology Fast Forward. Published on February 18, 2005 as DOI: 10.1124/mol.105.010959
This article has not been copyedited and formatted. The final version may differ from this version.

exponential for extrapolation of initial slope, and normalizing for total fluorescence (background-subtracted initial fluorescence). All compound plates contained negative controls (DMSO vehicle alone) and positive controls (genistein, 5 and 50 μM). Assay analysis indicated a Z'-factor (Zhang et al., 1999) of > 0.7.

Synthetic chemistry – ^{1}H spectra were obtained in $CDCl_3$ or d_6-DMSO using a Mercury 400 MHz spectrometer. Flash column chromatography was done using EM silica gel (230-400 mesh). Thin layer chromatography was carried out on Merk silica gel 60 F254 plates and visualized under a UV lamp. Microwave reactions were carried out on an Emrys synthesizer. Representative synthetic schemes for a phenylglycine and sulfonamide follow (see Fig. 2A).

For synthesis of PG-01, to a solution of *N*-*tert*-butoxycarbonyl-*N*-methylphenylgycine (**I**) (1.26 g, 4.75 mmol) at room temperature was added *p*-isopropylaniline (705 mg, 5.22 mmol), 4-(N,N-dimethylamino) pyridine (DMAP) (116 mg, 0.92 mmol) in CH_2Cl_2 (25 mL), and 1-ethyl-3-[3-(dimethylamino)-propyl]carbodiimide (EDCI, 1.00 g, 5.22 mmol). The reaction mixture was stirred for 2 h and then quenched by pouring over saturated NH_4Cl. After extraction with CH_2Cl_2 the organic layer was washed successively with water and brine, dried (Na_2SO_4), and concentrated *in vacuo*. Column chromatography of the crude residue gave [(4-isopropylphenylcarbamoyl)-phenylmethyl]-methylcarbamic acid *tert*-butyl ester (**IIA**) as a white solid (1.67 g, 92%). **IIA** (300 mg, 0.785 mmol) was dissolved in a minimal quantity of trifluoroacetic acid (TFA), maintained at room temperature for 15 min, poured over aqueous $NaHCO_3$, and extracted with CH_2Cl_2. Washing, drying and evaporation of the organic layer gave **II** as a yellow oil (218 mg, 98%). To a mixture of **II** (177 mg, 0.620 mmol), indole-3-acetic acid (114 mg, 0.651 mmol) and DMAP (15 mg, 0.124 mmol) in CH_2Cl_2 (5 mL), EDCI (131 mg, 0.682 mmol) was added at room temperature. The reaction mixture was worked up as for **IIA** and recrystallized from CH_2Cl_2 : MeOH (9:1) to give PG-01 as a white solid (1.67 g, 92%). Mass (ES+): M/Z = 440 $[M+1]^+$; ^{1}H NMR δ 1.21 (d, 6H, *J* = 6.9 Hz), 2.85 (sep, 1H, *J* = 6.9 Hz), 2.95 (s, 3H), 3.91 (s, 2H), 6.55 (s, 1H), 7.08-7.40 (m, 13H), 7.59 (d, 1H, *J* =7.8 Hz), 7.88 (bs, 1H), 8.13 (bs, 1H).

For synthesis of SF-03, compound **III** (Blus, 1999) (2.21 g, 8.0 mmol) and diethylethoxymethylenemalonate (1.81 g, 8.4 mmol) were dissolved in tetrahydrofuran (THF) (4 mL), and the solution was heated to 140 ^oC for 30 min until the THF and ethanol by-product evaporated. The residue was diluted with ethyl acetate (EtOAc), washed with brine, dried with Na_2SO_4, and evaporated to dryness. Flash chromatography gave light yellow solid **IIIB** (3.29 g, 90%). To a solution of phenyl ether (Ph_2O, 3 mL) and **IIIB** (130 mg, 0.30 mmol) in an Emrys microwave reaction vessel was added 4-chlorobenzoic acid (1 mg, 0.02 mmol). The solution was microwave irradiated at 250 ^{o}C for 75 min. The white precipitate was filtered and washed with hexane to yield **IV** (48 mg, 42%). To an Emrys microwave reaction vessel (0.2-0.5 mL) containing **IV** (65 mg, 0.083 mmol) was added *o*-methoxybenzyl amine (200 mg, 1.4 mmol) and microwave irradiated at 180 ^{o}C for 30 min. The resulting solution was diluted with dichloromethane and water, and extracted with EtOAc three times. After washing, drying and evaporation, the residue was purified by flash chromatography giving **SF-03** as a white powder (27 mg, 35%). Mass (ES+): M/Z = 492 $[M+1]^+$; 1H NMR $CDCl_3$ δ 1.08 (t, 3H, *J* = 7.2 Hz), 3.65 (q, 2H, *J* = 7.2 Hz), 3.79 (s, 3H), 4.70 (d, 2H, *J* = 6.0 Hz), 6.81 (m, 2H), 7.02 (m, 2H), 7.16 (td, 1H, *J* = 8.0, 1.6 Hz), 7.23 (d, 1H, *J* = 7.2 Hz), 7.29 (m, 2H), 7.37 (d, 1H, *J* = 8.4 Hz), 7.53 (dd, 1H, *J* = 8.8, 2.0 Hz), 8.77 (d, 1H, *J* = 2.0 Hz), 8.83 (d, 1H, *J* = 6.4 Hz), 10.74 (t, 1H, *J* = 5.6 Hz), 12.30 (d, 1H, *J* = 4.4 Hz).

Assays of cAMP – cAMP activity was measured using the BIOTRAK enzymatic immunoassay (Amersham) on FRT cell lysates after incubation with activators for 10 min in the presence of 0.5 µM forskolin.

Short-circuit current measurements – For Ussing chamber experiments ΔF508-CFTR expressing FRT cells were seeded on Snapwell inserts and cultured for 7-9 days. The basolateral solution contained (in mM): 130 NaCl, 2.7 KCl, 1.5 KH_2PO_4, 1 $CaCl_2$, 0.5 $MgCl_2$, 10 glucose, 10 Na-Hepes (pH 7.3). In the apical bathing solution 65 mM NaCl was replaced by Na gluconate, and $CaCl_2$ was increased to 2 mM. Solutions were bubbled with air and maintained at 37 °C. The basolateral membrane was permeabilized with 250 µg/ml amphotericin B. For human bronchial epithelial cells, apical and basolateral chambers contained 126 mM NaCl, 0.38 mM KH_2PO_4, 2.1 mM K_2HPO_4, 1 mM $MgSO_4$, 1 mM $CaCl_2$, 24 mM $NaHCO_3$ and 10 mM glucose (basolateral membrane not permeabilized). Hemichambers were connected to a DVC-1000 voltage clamp (World Precision Instruments) via Ag/AgCl electrodes and 1 M KCl agar bridges for recording short-circuit current.

***Patch-clamp analysis* –** Experiments were performed in the cell-attached configuration of the patch-clamp technique on FRT cells expressing ΔF508-CFTR. Cells were plated at a density of 10^4 cells/well and, grown at 37 ^{o}C for 24-48 hours, and then incubated for 24-48 hours at 27 °C to allow trafficking of the ΔF508 protein to the plasma membrane.

Single channel recordings were obtained using an EPC-7 patch-clamp amplifier (List Medical). Data were filtered at 250 Hz and digitized at 500 Hz using an ITC-16 data translation interface (Instrutech). The pipette solution contained (in mM): 120 CsCl, 10 TEA-Cl, 0.5 EGTA, 1 $MgCl_2$, 40 mannitol, 10 Cs-HEPES (pH 7.3). The bath solution contained (in mM): 130 KCl, 2 NaCl, 2 $CaCl_2$, 2 $MgCl_2$, 10 glucose, 20 mannitol, 10 Na-HEPES (pH 7.3). Channel activity in the patches was recorded before and after stimulation with forskolin (20 µM), with and without potentiators. Most experiments were done with a pipette voltage of –60 mV (referred to the bath). Analysis of open channel probability (P_o), mean channel open time (T_o), and mean channel closed time (T_c) was done using recordings of at least 3 min as described (Taddei et al., 2004).

***Pharmacokinetics* –** To increase compound solubility, potentiators were dissolved in a liposomal formulation containing 5 mg potentiator in 21.3 mg hydrogenated soy phosphatidylcholine, 5.2 mg cholesterol, 8.4 mg distearoylphosphatidylglycerol, and 90 mg sucrose in 5 ml PBS. A bolus of potentiator-containing solution (5 mg/kg) was administered intravenously in rats over 1 min (male Sprague-Dawley rats, 360-420 grams) by a jugular vein catheter. Arterial blood samples (~1 ml) were obtained at predetermined times for LCMS analysis. Animal procedures were approved by the U.C.S.F. Committee on Animal Research.

***Liquid chromatography / mass spectrometry (LCMS)* –** For analysis of blood samples, collected plasma was chilled on ice, and ice-cold acetonitrile (2:1 v:v) was added to precipitate proteins. Samples were centrifuged at 4 ^{o}C at 20,000g for 10 min. Supernatants (supplemented with sulforhodamine 101 as internal standard) were analyzed for PG-01 and SF-03

Molecular Pharmacology Fast Forward. Published on February 18, 2005 as DOI: 10.1124/mol.105.010959
This article has not been copyedited and formatted. The final version may differ from this version.

by extraction with C-18 reversed-phase cartridges (1 ml, Alltech Associates, Inc. Deerfield, IL) by standard procedures. The eluate was evaporated, and the residue was reconstituted in 100 µl of mobile phase for HPLC analysis. Reversed-phase HPLC separations were carried out using a Supelco C18 column (2.1 x 100 mm, 3 µm particle size) connected to a solvent delivery system (Waters model 2690, Milford, MA). The solvent system consisted of a linear gradient from 20% CH_3CN/10 mM KH_2PO_4, pH 3 to 95% CH_3CN/10mM KH_2PO_4, pH 3 over 10 min, followed by 6 min at 95% CH_3CN/20 mM NH_4OAc (0.2 ml/min flow rate). PG-01 and SF-03 were detected at 256 nm, after establishing a linear standard calibration curve in the range of 20-5000 nM. The detection limit was 10 nM and recovery was >90%. Mass spectra were acquired on a mass spectrometer (Alliance HT 2790 + ZQ) using negative ion detection, scanning from 200 to 800 Da as described (Sonawane et al., 2004).

***Stability in hepatic microsomes* –** PG-01 and SF-03 (10 µM each) were incubated separately with a phosphate buffered (100 mM) solution of rat liver microsomes (2 mg protein/ml, Sigma) containing NADPH (0 or 1 mM) for 60 min at 37 ^{o}C. After 60 min the mixture was chilled on ice, and 0.5 ml of ice-cold acetonitrile was added to precipitate the proteins for LCMS analysis as described above.

RESULTS

Compounds were screened at a concentration of 2.5 µM (in the presence of forskolin, 20 µM) in ΔF508-CFTR expressing FRT cells after low temperature rescue. CFTR-dependent I^- influx was determined from the time course of decreasing cellular YFP fluorescence. The screening revealed many compounds that at 2.5 µM increased I^- influx as much as the reference compound genistein at 50 µM, and substantially greater than forskolin (20 µM) alone (Fig. 1A). Most of these active compounds had phenylglycine (PG) and sulfonamide (SF) scaffolds (Fig. 1B); in addition, some active compounds were related structurally to tetrahydrobenzothiophene potentiators identified previously (Yang et al., 2003). Dose-response analysis of more 1,000 analogues of each chemical class not included in the primary library established a structure-activity relationship data base. An example of dose-response analysis of phenylglycine analogs is

Molecular Pharmacology Fast Forward. Published on February 18, 2005 as DOI: 10.1124/mol.105.010959
This article has not been copyedited and formatted. The final version may differ from this version.

shown in Fig. 1C, with compounds having a wide range of activating potencies. Dose-response data from the fluorescence assay for the most active compound of each class is shown in Fig. 1D, with data for comparison shown for genistein and the tetrahydrobenzothiophene $\Delta F508_{act}$-02. Activation of ΔF508-CFTR was confirmed for each of the compounds by showing no activity on non-transfected FRT cells, and near complete inhibition of the increased I^- influx by the thiazolidinone $CFTR_{inh}$-172 (Ma et al., 2002a) at 10 µM (not shown).

Table 1 summarizes structure-activity relationship (SAR) data for the most potent PG and SF analogs; data for a larger series of less active analogs is provided in S*upplemental information.* Fig. 2B summarizes the principle conclusions from SAR analysis. Active PGs contained a disubstituted glycyl amine with amide of aromatic amines. Substitutions at R1 had relatively little effect on compound activity. Most active compounds had as R1 4-isopropylphenyl, with reduced activity for R1 as 2,3-diH-1,4-benzodioxin-6-yl in (PG-02, -04) or 4-methoxyphenyl (PG-05). Evaluation of R2 substitutions indicated that replacement of hydrogen by methyl (PG-07) or methoxy (PG10) strongly reduced potency. The R2 phenyl group appeared to be important for activity as its replacement by indol-3-methyl reduced activity. All potent compounds had as R3 a methyl, as its replacement by hydrogen (PG-06) or furfuryl-2-methyl reduced activity. Most active compounds had as R4 an indolyl-3-acetyl, as substitution by thiophene-2-acetyl or diphenyl acetyl resulted in loss of activity. Thus, greatest ΔF508-CFTR activating potency was produced by hydrophobic R1, R2, and R3, with R4 as indolyl-2 (or 3)-acetyl.

SAR analysis of sulfonamides supported the requirement of 3-carboxamide and 6-aminosulfo groups. All active quinolone compounds had as R1 hydrophobic groups such as alkoxy, dialkyl, alkyl, and halo substituted phenyl or cyclohexyl (SF-10) groups. Greatest activity was found for R2 as non-polar alkyl chains (ethyl, methyl, 2-propenyl). The most potent compounds (SF-02 to -04) contained an ethyl group at R2 in combination with phenyl as R1, and an alkyl group as R3. Substitutions at R3 with non-polar linear or branched alkyl or cycloalkyl groups improved activity. In general, greatest potency was found with hydrophobic-nonpolar substitutions on sulfonamide and carboxamide moieties.

Apical membrane current in FRT cells was measured to verify activation of ΔF508-CFTR Cl^- conductance and to determine compound potency. Apical membrane current was measured after permeabilization of the basolateral membrane with amphotericin B in the presence of a Cl^- gradient (apical 65 mM Cl^-, basolateral 130 mM). After maximal forskolin (20 µM), test compounds were added at increasing concentrations as shown in Fig. 3A, followed by $CFTR_{inh}$-172. The small effect of forskolin alone demonstrated defective ΔF508-CFTR gating, as ten-fold lower concentrations of forskolin fully activate wildtype CFTR in this assay (Galietta et al., 2001c). PG-01 and SF-01 gave ΔF508-CFTR Cl^- currents with potencies better than 100 nM (Fig. 3B), and maximal currents comparable to or greater than that produced by 50 µM genistein. Interestingly, these compounds were substantially less effective for activation of wildtype CFTR. When stimulated with submaximal forskolin, PG-01 and SF-01 produced only a fraction (40-60%) of the current elicited by genistein (not shown).

Experiments were also done by adding the potentiator first, followed by increasing concentrations of forskolin. Forskolin alone at 0.5 and 2 µM gave little apical membrane current (Fig. 3C, top left). However, PG-01, which did not itself activate ΔF508-CFTR, produced substantial ΔF508-CFTR Cl^- current after addition of 0.5 and 2 µM forskolin (Fig. 3C, bottom left). Data are summarized in Fig. 3C (right), showing significant synergy of these potentiators with forskolin. The correction of ΔF508-CFTR gating in the presence of relatively low concentrations of cAMP agonists is a desirable property of these compounds (see Discussion).

An initial analysis of compound specificity was done. Cells were incubated with potentiators in the presence of a low concentration of forskolin (0.5 µM), lysed, and assayed for cAMP. PG-01 and SF-01 did not increase cAMP above the level induced by forskolin 0.5 µM alone (Fig. 4A), whereas the compound $CFTR_{act}$-16, an indirect activator of CFTR (Ma et al., 2002b), strongly increased cAMP. MDR-1 activity was assayed by intracellular accumulation of the fluorescent probe rhodamine 123. Two cell lines were used, the parental human tracheal cell line 9HTEo-, and its multidrug resistant subclone 9HTEo-/Dx that strongly expresses MDR-1 (Rasola et al., 1994). 9HTEo-/Dx cells accumulate much less rhodamine 123 than 9HTEo- cells as a consequence of MDR-1 mediated dye extrusion. Dye accumulation was increased significantly by the MDR-1 inhibitor verapamil, but was not affected by PG-01 or SF-01 (Fig. 4B). Last, effects on the UTP/calcium activated Cl^- channel were measured from short circuit current measurements on human bronchial epithelial cells. There was no effect of PG-01 or SF-01 on the magnitude or kinetics of the calcium-activated Cl^- current (Fig. 4C).

The ΔF508-CFTR activating mechanism was investigated by cell-attached patch-clamp measurements. Addition of 20 µM forskolin produced low channel activity with a P_o of 0.04 (Fig. 5A). Channel openings were separated by long duration closures, in agreement with previous observations on ΔF508-CFTR (Dalemans et al., 1991; Haws et al., 1996). Although all patches contained more than one channel, simultaneous channel openings were rarely seen due to the low P_o. PG-01 or SF-01 at 100 nM strongly stimulated channel activity with multiple channel openings observed. P_o after activation (0.3-0.4) was comparable to that of wildtype CFTR (Dalemans et al., 1991; Haws et al., 1996) (Fig. 5B). Analysis of gating kinetics indicated that the increase in P_o was due to a reduction in mean channel closed time (T_c) rather than an increase in mean channel open time (T_o) (Fig. 5B).

The possibility was evaluated that the PG or SF ΔF508-CFTR potentiators might correct defective gating in other mutant CFTRs that cause CF in humans. Measurements were done in the 'class III' mutants G551D and G1349D, which produce a severe gating defect without impairment in protein trafficking (Gregory et al., 1991). These mutations affect the glycine residues in NBD1 and NBD2 that are highly conserved in ATP-binding cassette proteins (Hyde et al., 1990; Logan et al., 1994). The G551D and G1349D mutant CFTRs produced little Cl^- current after addition of maximal forskolin (Figs. 6A and 6B). Genistein, a known activator of G551D- and G1349D-CFTR, increased Cl^- current substantially, albeit at high micromolar concentrations (Figs. 6A and 6B, top curves). PG-01 produced large currents in both G551D- and G1349D-CFTR expressing cells as shown in Figs. 6A and 6B (bottom curves), and summarized in Figs. 6C and 6D. The currents were sensitive to $CFTR_{inh}$-172 and not seen in non-transfected cells. In contrast to PG-01, SF-01 and the benzothiophene $\Delta F508_{act}$-02 did not increase Cl^- currents in G551D- and G1349D-CFTR expressing cells (not shown).

The ability of PG-01 and SF-01 to correct defective CFTR channel gating in CF human airway epithelial cells was tested (Fig. 7). Human nasal epithelial cells from ΔF508 homozygote subjects were cultured as polarized monolayers on permeable supports for transepithelial short-circuit current measurement. After blocking the epithelial Na^+ channel with amiloride, forskolin (20 µM) was applied, followed by genistein, PG-01, or SF-01. $CFTR_{inh}$-172 was applied at the end of each study to determine total CFTR-dependent current. Cells maintained at 37 °C had little CFTR current, in agreement with the expected intracellular retention of ΔF508-CFTR. Low temperature rescue by incubation at 27 °C for 20-24 hours produced greater ΔF508-CFTR current, with significant activation by PG-01 and SF-01 at nanomolar concentrations (Fig. 7A). Stimulation by forskolin plus PG-01 or SF-01 was blocked by $CFTR_{inh}$-172. Genistein was comparably effective but at much higher concentrations. Primary cell cultures from subjects carrying CFTR mutations causing pure gating defects were also tested. For these studies cells were cultured at 37 °C. Nasal epithelial cells from a subject with the G551D mutation (Zegarra et al., 2002) showed a large response to PG-01 after forskolin stimulation (Fig. 7B). Cells were also tested from a subject having D1152H and ΔF508 CFTR mutations, the former mutation affecting the second nucleotide binding domain and causing a decrease in channel activity (Vankeerberghen et al., 1998). The D1152H/ΔF508 cells maintained at 37 °C cells showed large CFTR currents in response to PG-01 (Fig. 7C).

To predict hepatic clearance of PG-01 and SF-03, *in vitro* incubations were done with rat hepatic microsomes for 1 hr at 37 ^{o}C in the absence (control) and presence of NADPH, followed by LCMS analysis. SF-03 was chosen for these studies as the most potent of the SF compounds. Fig 8A (*top, left and right*) shows representative HPLC chromatograms, with PG-01 eluting at 7.85 min, and its two major metabolites (M1 and M2) eluting at 7.16 and 6.88 min. Mass spectrometry identified the original compound, and M1 and M2 with m/z 456 (~PG-01+OH; $[M+1]^+$) and 472 (~PG-01+2OH; $[M+1]^+$), respectively (Fig 8A, *top*, *middle*). A minor metabolite was also detected at 7.43 min with m/z 428. Approximately 90 % of the PG-01 was metabolized after incubation with microsomes for 1 h in the presence of NADPH, and non-metabolized PG-01 was not detectable after 2 h (not shown). Fig. 8A (*bottom, left and right*) shows the HPLC profile for SF-03 and its two major metabolites eluting at 7.44 min and 7.16 / 6.77 min, respectively, with corresponding molecular ion peaks (Fig. 8A, *bottom*, *middle*) at m/z 492 (SF-03, $[M+1]^+$), 508 (~SF-03+OH, $[M+1]^+$) and 389. SF-03 was ~35 % degraded after a 1 h incubation with liver microsomes in presence of NADPH.

Pharmacokinetic analysis of PG-01 and SF-03 in rats was done by serial measurements of plasma concentrations after single bolus infusions (5 mg/Kg). Fig. 8B (*left*) shows HPLC chromatograms for PG-01 and SF-03 (each at 50 nM added to control plasma and supplemented with sulforhodamine 101 as internal standard), demonstrating the sensitivity of

Molecular Pharmacology Fast Forward. Published on February 18, 2005 as DOI: 10.1124/mol.105.010959
This article has not been copyedited and formatted. The final version may differ from this version.

the assay. PG-01 pharmacokinetics fitted a two-compartment model with half-times of <5 min and 130 min, with volume of distribution ~4 L, whereas SF-03 clearance had elimination half-times of ~7 and 110 min, with volume of distribution ~2 L (Fig. 8B, *right*).

DISCUSSION

The purpose of this study was to identify new classes of drug-like compounds that strongly activate CF-causing mutant CFTRs. Our strategy was to carry out high-throughput screening for ΔF508-CFTR potentiators utilizing a collection of 50,000 diverse, drug-like small molecules. The screening yielded two novel classes of ΔF508-CFTR potentiators having phenylglycine and sulfonamide scaffolds. Several rounds of optimization involving testing of analogs of each compound class produced ΔF508-CFTR potentiators that fully activated ΔF508-CFTR with potencies better than 100 nM. Many active phenylglycine and sulfonamide analogs of widely differing activities were identified, which is an important prerequisite for development of these compounds as drugs to treat CF. Analysis of phenylglycine properties revealed a number of favorable properties, including the ability to correct defective channel gating in several different CFTR mutants and synergy with cAMP agonists. The phenylglycine PG-01 was metabolized rapidly in hepatic microsomes, suggesting the possibility of aerosol delivery for CF therapy in which any absorbed compound would be inactivated rapidly by hepatic metabolism. The sulfonamides were relatively stable metabolically and did not correct defective gating in non-ΔF508 CFTR mutants, though they did show synergy with cAMP agonists.

Measurement of transepithelial chloride current in FRT cells confirmed correction of defective ΔF508-CFTR gating by the phenylglycine and sulfonamide compounds. In one protocol, cells were stimulated with maximal forskolin, followed by increasing concentrations of test compounds. Total current activated by forskolin plus potentiators was blocked by $CFTR_{inh}$-172. In a different protocol, a dose-response to forskolin was done with vs. without prior potentiator addition. Little response to forskolin was seen in the absence of potentiator, and only at high forskolin concentrations. Addition of the potentiator first, which did not itself activate ΔF508-CFTR, restored substantial sensitivity to forskolin. Measurements of cellular cAMP concentrations indicated that the apparent synergy of the potentiators with forskolin is

Molecular Pharmacology Fast Forward. Published on February 18, 2005 as DOI: 10.1124/mol.105.010959
This article has not been copyedited and formatted. The final version may differ from this version.

not due to cAMP elevation. We propose a direct interaction between the phenylglycine and sulfonamide potentiators with ΔF508-CFTR. The lack of effect of these compounds in the absence of cAMP elevating agents and the apparent synergy with cAMP elevating agents are favorable properties in that near-native CFTR regulation is recapitulated.

Cell attached patch-clamp experiments were carried out to investigate the mechanism of channel activation. In the presence of forskolin alone, ΔF508-CFTR produced bursts of channel openings separated by long closures lasting for several seconds, resulting in reduced open channel probability. The potentiators strongly increased channel activity, remarkably reducing the time spent in the closed state. The resulting open channel probability was comparable to that of wildtype CFTR.

The phenyglycines corrected defective gating in a number of CF-causing CFTR mutants including ΔF508, G551D, G1349D and D1152H. G551D and G1349D affect critical glycine residues in nucleotide binding domains 1 and 2 of CFTR, respectively (Hyde et al., 1990), producing a severe gating defect (Gregory et al., 1991; Logan et al., 1994; Zegarra-Moran et al., 2002; Derand et al., 2002). Forskolin alone produced little activation of these mutant CFTRs even at high concentrations, whereas PG-01 after forskolin produced a >10-fold elevation in current. The apparent K_d for PG-01 for G551D-CFTR activation was ~1 µM, approximately 100-fold better than that of genistein. The potency for activation G1349D-CFTR by PG-01 was even better, ~ 40 nM. In contrast to ΔF508, other cystic fibrosis mutations, of which more than 1000 have been identified, have a relatively very low frequency. The fraction of CF mutations that cause a pure gating defect (class III mutants) is unknown but is likely to be substantial. The phenylglycines may be useful in mono-drug therapy for many of these mutations. Further studies are warranted to establish the molecular mechanism by which a small molecule is able to correct defective channel gating in quite different CFTR mutants.

Transepithelial current measurements on primary cultures of human airway epithelia indicated that the phenylglycine and sulfonamide potentiators identified here are also effective in a native epithelium. This finding is not unexpected since these compounds probably bind to mutant CFTRs directly, and so their activity should be cell-context independent. The best phenylglycine was also effective on cells cultured from CF subjects having G551D and D1152H CFTR mutations, supporting the possible use of this class of compounds for mono-therapy of CF caused by some mutations. For therapy of CF caused by the ΔF508-CFTR mutation, the potentiators would probably need to be combined with compounds that correct defective ΔF508-CFTR cellular processing.

Acknowledgments:

We thank Drs. R. Kip Guy and A. Shelat for computational analysis for compound selection, and for advice on SAR analysis.

REFERENCES

Blus, K (1999) Synthesis and properties of acid dyes derived from 7-amino-1-hydroxynaphthalene-3-sulfonic acid. *Dyes and Pigments* **41:**149-157.

Bobadilla J, Macek M, Fine JP, and Farrell PM (2002) Cystic fibrosis: a worldwide analysis of CFTR mutations-correlation with incidence data and application to screening. *Hum Mutat* **19:**575-606.

Cashman SM, Patino A, Delgado MG, Byrne L, Denham B, and Dearce M (1995) The Irish cystic fibrosis database. *J Med Genet* **32:**972-975.

Dalemans W, Barbry P, Champigny G, Jallat S, Dott K, Dreyer D, Crystal RG, Pavirani A, Lecocq JP, and Lazdunski M (1991) Altered chloride ion channel kinetics associated with the ΔF508 cystic fibrosis mutation. *Nature* **354:**526-528.

Denning GM, Anderson MP, Amara JF, Marshall J, Smith AE, and Welsh MJ (1992) Processing of mutant cystic fibrosis transmembrane conductance regulator is temperature-sensitive. *Nature* **358:**761-764.

Derand R, Bulteau-Pignoux L, and Becq F (2002) The cystic fibrosis mutation G551D alters the non-Michaelis-Menten behavior of the cystic fibrosis transmembrane conductance regulator (CFTR) channel and abolishes the inhibitory genistein binding site. *J Biol Chem* **277:**35999-36004.

Drumm ML, Wilkinson DJ, Smit LS, Worrell RT, Strong TV, Frizzell RA, Dawson DC, and Collins FS (1991) Chloride conductance expressed by ΔF508 and other mutant CFTRs in Xenopus oocytes. *Science* **254:**1797-1799.

Galietta LJV, Haggie PM, and Verkman AS (2001a) Green fluorescent protein-based halide indicators with improved chloride and iodide affinities. *FEBS Lett* **499:**220-224.

Galietta LJV, Springsteel MF, Eda M, Niedzinski EJ, By K, Haddadin MJ, Kurth MJ, Nantz MH, and Verkman AS (2001b) Novel CFTR chloride channel activators identified by screening of combinatorial libraries based on flavone and benzoquinolizinium lead compounds. *J Biol Chem* **276:**19723-19728.

Galietta LJV, Jayaraman S, and Verkman AS (2001c) Cell-based assay for high-throughput quantitative screening of CFTR chloride transport agonists. *Am J Physiol* **281:**C1734-C1742.

Galietta LJV, Musante L, Romio L, Caruso U, Fantasia A, Gazzolo A, Romano L, Sacco O, Rossi GA, Varesio L, and Zegarra-Moran O (1998) An electrogenic amino acid transporter in the apical membrane of cultured human bronchial epithelial cells. *Am J Physiol* **275:**L917-L923.

Gregory RJ, Rich DP, Cheng SH, Souza DW, Paul S, Manavalan P, Anderson MP, Welsh MJ, and Smith AE (1991) Maturation and function of cystic fibrosis transmembrane conductance regulator variants bearing mutations in putative nucleotide-binding domains 1 and 2. *Mol Cell Biol* **11:**3886-3893.

Molecular Pharmacology Fast Forward. Published on February 18, 2005 as DOI: 10.1124/mol.105.010959
This article has not been copyedited and formatted. The final version may differ from this version.

Hamosh A, King TM, Rosenstein BJ, Corey M, Levison H, Durie P, Tsui LC, McIntosh I, Keston M, Brock DJH, Macek Jr M, Zemkova D, Krasnicanova H, Vavrova V, Macek Sr M, Golder N, Schwartz MJ, Super M, Watson EK, Williams C, Bush A, O'Mahoney SM, Humphries P, Dearce MA, Reis A, Burger J, Stuhrmann M, Schmidtke J, Wulbrand U, Dork T, Tummler B, and Cutting GR (1992) Cystic Fibrosis patients bearing the common missense mutation Gly to Asp at codon 551 and the ΔF508 mutation are clinically indistinguishable from ΔF508 homozygotes, except for a decreased risk of meconium ileus. *Am J Hum Genet* **51:**245-250.

Haws CM, Nepomuceno IB, Krouse ME, Wakelee H, Law T, Xia Y, Nguyen H, and Wine JJ (1996) ΔF508-CFTR channels: kinetics, activation by forskolin, and potentiation by xanthines. *Am J Physiol* **270:**C1544-C1555.

Hwang T-C, Wang F, Yang I, and Reenstra WW (1997) Genistein potentiates wild-type and ΔF508-CFTR channel activity. *Am J Physiol* **273:**C988-C998.

Hyde SC, Emsley P, Hartshorn MJ, Mimmack MM, Gileadi U, Pearce SR, Gallagher MP, Gill DR, Hubbard RE, and Higgins CF (1990) Structural model of ATP-binding proteins associated with cystic fibrosis, multidrug resistance and bacterial transport. *Nature* **346:**362-365.

Illek B, Zhang L, Lewis NC, Moss RB, Dong JY, and Fischer H (1999) Defective function of the cystic fibrosis-causing mutation missense mutation G551D is recovered by genistein. *Am J Physiol* **277:**C833-C839.

Jensen TJ, Loo MA, Pind S, Williams DB, Goldberg AL, and Riordan JR (1995) Multiple proteolytic systems, including the proteasome, contribute to CFTR processing. *Cell* **83:**129–135.

Kopito RR (1999) Biosynthesis and degradation of CFTR. *Physiol Rev* **79:**S167-S173.

Logan J, Hiestand D, Daram P, Huang Z, Muccio DD, Hartman J, Haley B, Cook WJ, Sorscher EJ (1994) Cystic fibrosis transmembrane conductance regulator mutations that disrupt nucleotide binding. *J Clin Invest* **94:**228-236.

Ma T, Thiagarajah JR, Yang H, Sonawane ND, Folli C, Galietta LJ, and Verkman AS (2002a) Thiazolidinone CFTR inhibitor identified by high-throughput screening blocks cholera-toxin induced intestinal fluid secretion. *J Clin Invest* **110:**1651-1658.

Ma T, Vetrivel L, Yang H, Pedemonte N, Zegarra-Moran O, Galietta LJV, and Verkman AS (2002b) High-affinity activators of cystic fibrosis transmembrane conductance regulator (CFTR) chloride conductance identified by high-throughput screening. *J Biol Chem* **277:**37235-37241.

Penque D, Mendes F, Beck S, Farinha C, Pacheco P, Nogueira P, Lavinha J, Malho R, and Amaral MD (2000) Cystic fibrosis F508del patients have apically localized CFTR in a reduced number of airway cells. *Lab Invest* **80:**857-868.

Molecular Pharmacology Fast Forward. Published on February 18, 2005 as DOI: 10.1124/mol.105.010959
This article has not been copyedited and formatted. The final version may differ from this version.

Pilewski JM and Frizzell RA (1999) Role of CFTR in airway disease. *Physiol Rev* **79:**S215-S255.

Rasola A, Galietta LJV, Gruenert DC, and Romeo G (1994) Volume-sensitive chloride currents in four epithelial cell lines are not directly correlated to the expression of the MDR-1 gene. *J Biol Chem* **269:**1432-1436.

Sermet-Gaudelus I, Vallee B, Urbin I, Torossi T, Marianovski R, Fajac A, Feuillet MN, Bresson JL, Lenoir G, Bernaudin JF, and Edelman A (2002) Normal function of the cystic fibrosis conductance regulator protein can be associated with homozygous ΔF508 mutation. *Pediatr Res* **52:**628-635.

Sheppard DN and Welsh MJ (1999) Structure and function of the CFTR chloride channel. *Physiol Rev* **79:**S23-S45.

Sonawane ND, Muanprasat C, Nagatani R, Song Y, and Verkman AS (2004) In vivo pharmacology and antidiarrheal efficacy of a thiazolidinone CFTR inhibitor in rodents. *J Pharm Sci* **94:**134-143.

Taddei A, Folli C, Zegarra-Moran O, Fanen P, Verkman AS, and Galietta LJV (2004) Altered channel gating mechanism for CFTR inhibition by a high-affinity thiazolidinone blocker. *FEBS Lett* **558:**52-56.

Vankeerberghen A, Wei L, Teng H, Jaspers M, Cassiman JJ, Nilius B, and Cuppens H (1998) Characterization of mutations located in exon 18 of the CFTR gene. *FEBS Lett* **437:**1-4.

Ward CL, Omura S, and Kopito RR (1995) Degradation of CFTR by the ubiquitin-proteasome pathway. *Cell* **83:**121-127.

Yang H, Shelat AA, Guy RK, Gopinath VS, Ma T, Du K, Lukacs GL, Taddei A, Folli C, Pedemonte N, Galietta LJV, and Verkman AS (2003) Nanomolar affinity small molecule correctors of defective ΔF508-CFTR chloride channel gating. *J Biol Chem* **278:**35079-35085.

Zegarra-Moran O, Romio L, Folli C, Caci E, Becq F, Vierfond JM, Mettey Y, Cabrini G, Fanen P, and Galietta LJV (2002) Correction of G551D-CFTR transport defect in epithelial monolayers by genistein but not by CPX or MPB-07. *Br J Pharmacol* **137:**504-512.

Zhang JH, Chung TD, and Oldenburg KR (1999) A simple statistical parameter for use in valuation and validation of high throughput screening assays. *J Biomol Screen* **4:**67-73.

Molecular Pharmacology Fast Forward. Published on February 18, 2005 as DOI: 10.1124/mol.105.010959
This article has not been copyedited and formatted. The final version may differ from this version.

Footnote to title:

This work was supported by the Cystic Fibrosis Foundation, and by grants HL73856, HL59198, EB00415, EY13574 and DK35124 from the National Institutes of Health. Dr. Galietta acknowledges grant GP0296Y01 from Telethon-Italy.

Reprint requests to:

Alan S. Verkman, M.D., Ph.D.

1246 Health Sciences East Tower

University of California, San Francisco

San Francisco, CA 94143-0521, U.S.A.

E-mail: verkman@itsa.ucsf.edu

Molecular Pharmacology Fast Forward. Published on February 18, 2005 as DOI: 10.1124/mol.105.010959
This article has not been copyedited and formatted. The final version may differ from this version.

FIGURE LEGENDS

Figure 1. Identification of ΔF508-CFTR potentiators by high-throughput screening. A. Original traces showing quenching of cellular YFP fluorescence by I^- addition with saline alone, and after additions of forskolin (20 µM) alone, or forskolin plus genistein (50 µM), SF-01 (2.5 µM) or PG-01 (2.5 µM). **B.** Chemical structures of potent phenylglycine (PG) and sulfonamide (SF) compounds. **C.** and **D.** Dose-response analysis of indicated compounds (mean ± SE, n=4), including the tetrahydrobenzothiophene $\Delta F508_{act}$-02 (Yang et al., 2003).

Figure 2. **Synthesis and structure-activity analysis of ΔF508-CFTR potentiators. A.** (top) Synthesis of phenylglycine PG-01. Conditions: a. *p*-isopropylaniline, EDCI, cat. (catalytic amount) DMAP, CH_2Cl_2, 22 ^oC, 2 h, yield 92%; b. TFA, 22 ^oC, 15 min, 98%; c. indole-3-acetic acid, EDCI, cat. DMAP, CH_2Cl_2, 22 ^oC, 2 h, 92%**.** (bottom) Synthesis of sulfonamide SF-03. Conditions: d. diethyl ethoxymethylene-malonate, 140 ^oC, 1 h, 95%; e. cat. *p*-chlorobenzoic acid. Ph_2O, 250 ^oC, 45%; f. *o*-methoxybenzyl-amine, neat, 180 ^oC, 35%. **B.** Conclusions from SAR analysis of PG and SF analogs. See results for explanations.

Figure 3. Activation of cell membrane Cl^- current by ΔF508-CFTR potentiators. Apical membrane Cl^- current measured in FRT cells expressing ΔF508-CFTR after low temperature rescue. **A.** Representative traces showing currents activated by forskolin (fsk, 20 µM) and ΔF508-CFTR potentiators PG-01 and SF-01, and inhibited by $CFTR_{inh}$-172. **B.** Average dose-responses for potentiators, with genistein data shown for comparison (SE, n=4). **C.** Representative curves (left) and averaged data (SE, n=4, right) from experiments showing forskolin dose-response with vs. without prior addition of potentiators (2 µM).

Figure 4. Specificity of ΔF508-CFTR potentiators. A. Intracellular cAMP concentration after forskolin addition without and with potentiators (2 µM). Effects of PG-01 and SF-01 not significant. **B.** MDR-1 activity shown as

Molecular Pharmacology Fast Forward. Published on February 18, 2005 as DOI: 10.1124/mol.105.010959
This article has not been copyedited and formatted. The final version may differ from this version.

rhodamine 123 accumulation in multidrug sensitive (9HTEo-) and multidrug resistant (9HTEo-/Dx) cells. Significant accumulation was found in 9HTEo-/Dx cells for verapamil (100 µM) but not for the potentiators (5 µM). **C.** Activation of Cl^- current by apical UTP in polarized human bronchial epithelia. Pretreatment with ΔF508-CFTR activators (2 µM) did not affect the maximum current or time-course of the UTP response.

Figure 5. Single-channel patch-clamp analysis of ΔF508-CFTR channel stimulation by potentiators. A. Representative recordings showing activity in multi-channel patches. Dotted line indicates current with channels closed. Pipette voltage was –60 mV. Downward deflections represent channel openings (Cl^- ions moving from pipette to cell). **B.** Mean open channel probability (P_o), mean closed time (T_c), and mean open time (T_o) in the presence of forskolin alone or in combination with indicated potentiators.

Figure 6. Activation of G551D- and G1349D-CFTR mutants. A. and **B.** Stimulation of apical membrane Cl^- current by genistein (top) and PG-01 (bottom) in G551D- and G1349D-CFTR expressing FRT cells. Cells were pretreated with forskolin (fsk, 20 µM). **C, D**. Dose-responses for the PG-01 and genistein for activation of G551D- and G1349D-CFTR (SE, n=4).

Figure 7. Stimulation of Cl^- secretion in CF human airway epithelial cells. Transepithelial short-circuit Cl^- current measured in response to genistein and indicated ΔF508-CFTR potentiators. **A.** Nasal epithelial cells from a ΔF508 homozygous patient. Cells were incubated at 27 °C for 24 h where indicated. **B.** G551D-CFTR cells. **C.** D1152H-CFTR cells.

Figure 8. Liquid chromatography / mass spectrometry analysis of microsomal metabolites of PG-01 and SF-03, and rat pharmacokinetics. A. Microsomes were incubated with PG-01 or SF-03 (each 10 µM) in the absence (control) or presence of NADPH for 1 hr at 37 ^{o}C, and processed as described under Methods. HPLC chromatograms at 256 nm

Molecular Pharmacology Fast Forward. Published on February 18, 2005 as DOI: 10.1124/mol.105.010959
This article has not been copyedited and formatted. The final version may differ from this version.

for control *(left)* and NADPH (*right*) samples, and corresponding ion current chromatograms for positive ion electrospray mass spectrometry for indicated m/z (*middle*). M1, metabolite 1; M2, metabolite 2. **B.** Pharmacokinetic analysis. *(left)* HPLC chromatogram of PG-01 and SF-03 demonstrating assay sensitivity to better than 50 nM. *(right)* Pharmacokinetics of PG-01 (*open circles*) and SF-03 (*filled circles*) after 5 mg/Kg intravenous bolus injection (mean ± SE, n=3-4 rats).

Molecular Pharmacology Fast Forward. Published on February 18, 2005 as DOI: 10.1124/mol.105.010959
This article has not been copyedited and formatted. The final version may differ from this version.

Table 1. Structure-activity relationship analysis of phenylglycine and sulfonamide ΔF508-CFTR potentiators

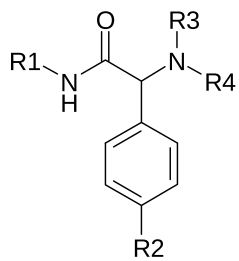

Phenylglycines (PG)

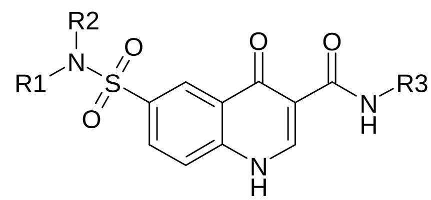

Sulfonamides (SF)

Compd.	R1	R2	R3	R4	Ka (μM)
PG-01	4-Isopropyl-Ph	H	Me	Indol-3-actyl	0.30
PG-02	2,3-diH-1,4-benzodioxin-6-yl	H	Me	Ac-NHCH$_2$CO-	0.30
PG-03	4-Isopropyl-Ph	4-OMe	Me	Indol-3-actyl	0.34
PG-04	2,3-diH-1,4-benzodioxin-6-yl	H	Me	Indol-3-acetyl	0.40
PG-05	4-OMe-Ph	H	Me	Indol-3-acetyl	0.70
PG-06	4-Isopropyl-Ph	H	H	Indol-3-acetyl	0.88
PG-07	1,3-benzodioxol-5-yl	4-Me	Me	Indol-3-acetyl	1.33
PG-08	4-OMe-Ph	4-OMe	Me	Indol-3-acetyl	2.13
PG-09	2,3-diH-1,4-benzodioxin-6-yl	4-Me	H	Indol-2-acetyl	2.33
PG-10	2,3-diH-1,4-benzodioxin-6-yl	4-OMe	Me	Indol-3-acetyl	2.71

Compd.	R1	R2	R3	Ka (μM)
SF-01	2-OEt-Ph	Me	2-propenyl	0.30
SF-02	Ph	Et	Cycloheptyl	0.02
SF-03	Ph	Et	2-OMe-Ph-methyl	0.03

Molecular Pharmacology Fast Forward. Published on February 18, 2005 as DOI: 10.1124/mol.105.010959
This article has not been copyedited and formatted. The final version may differ from this version.

SF-04	Ph	Et	Cyclohexyl	0.03
SF-05	OMe-Ph	Me	n-Pentyl	0.06
SF-06	Ph	2-propenyl	*n*-butyl	0.11
SF-07	Ph	2-propenyl	Cycloheptyl	0.12

Compd.	R1	R2	R3	Ka (μM)
SF-08	2,5-di-Me-Ph	Me	2-Pyridinylmethyl	0.13
SF-09	Ph	Et	(3-OMe)-propyl	0.14
SF-10	-CH_2-CH_2-CH(Me)-CH_2-CH_2-		3[(N-(*n*-butyl)phenylamino)propyl	0.14
SF-11	Ph	2-propenyl	2-Pyridinylmethyl	0.16
SF-12	Ph	2-Propenyl	n-Hexyl	0.19
SF-13	2-Me-Ph	Me	*n*-butyl	0.20
SF-14	2-EtO-Ph	Me	(Tetrahydro-2-furanyl)methyl	0.20
SF-15	3-Me-Ph	Me	n-pentyl	0.22
SF-16	Ph	Et	2-(1-cyclohexen-1-yl)ethyl	0.24
SF-17	Ph	Et	(Tetrahydro-2-furanyl)methyl	0.24
SF-18	2-Et-Ph	Me	2-Pyridinylmethyl	0.27
SF-19	2,5-di-Me-Ph	Me	3-OMe-propyl	0.29
SF-20	2,6-di-Me-Ph	Me	n-Butyl	0.33

Molecular Pharmacology Fast Forward. Published on February 18, 2005 as DOI: 10.1124/mol.105.010959
This article has not been copyedited and formatted. The final version may differ from this version.

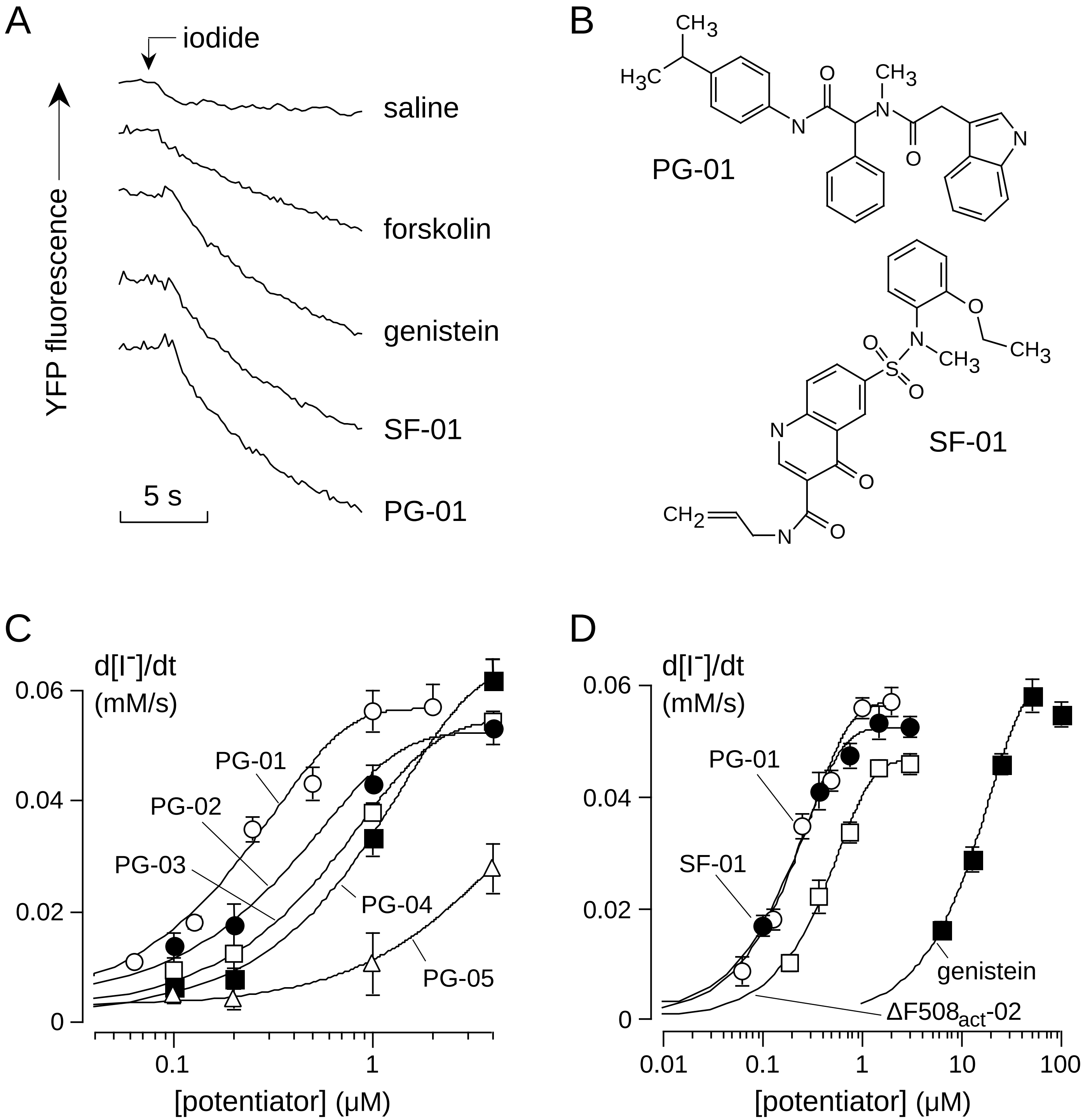

Figure 1

Molecular Pharmacology Fast Forward. Published on February 18, 2005 as DOI: 10.1124/mol.105.010959
This article has not been copyedited and formatted. The final version may differ from this version.

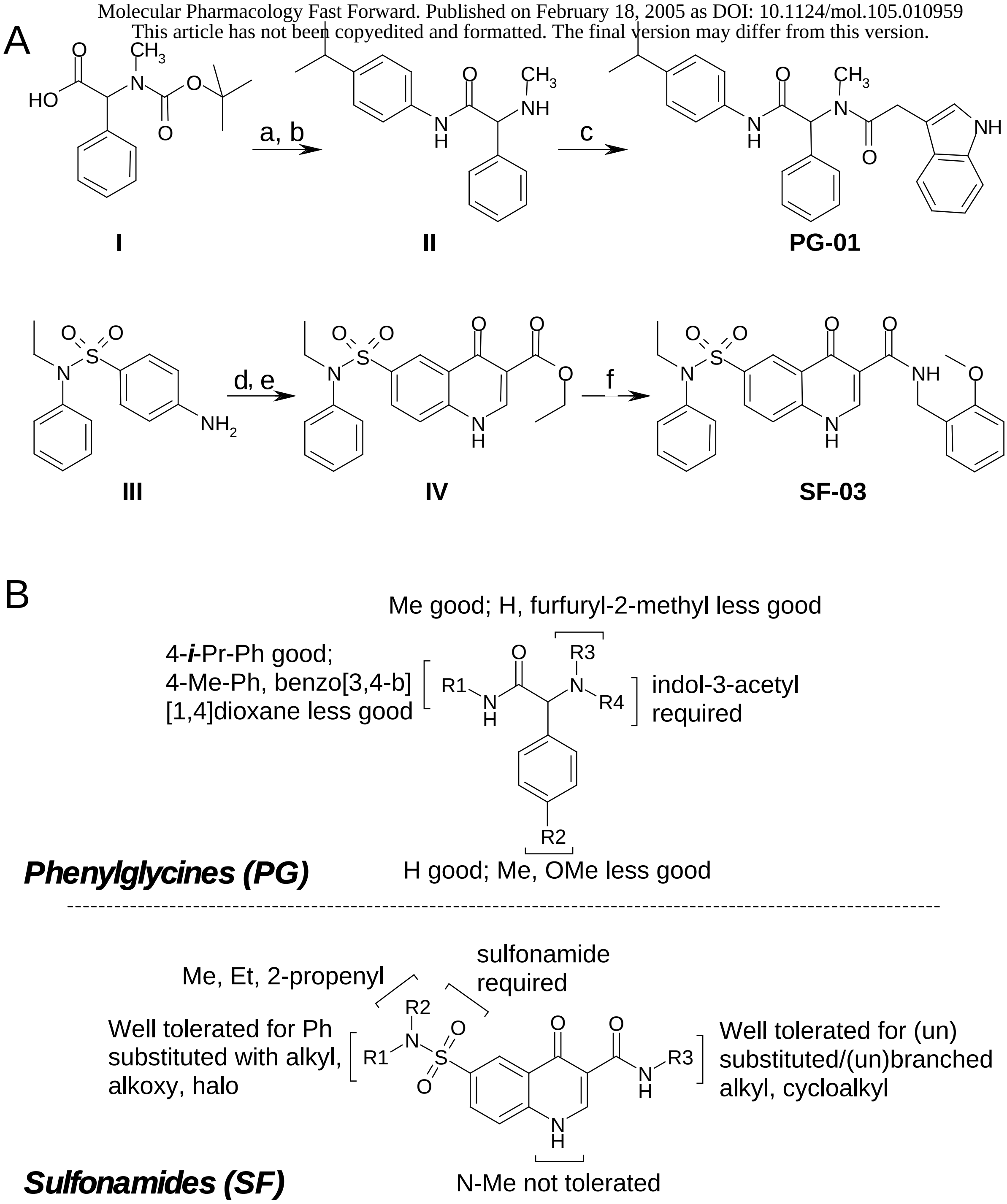

Figure 2

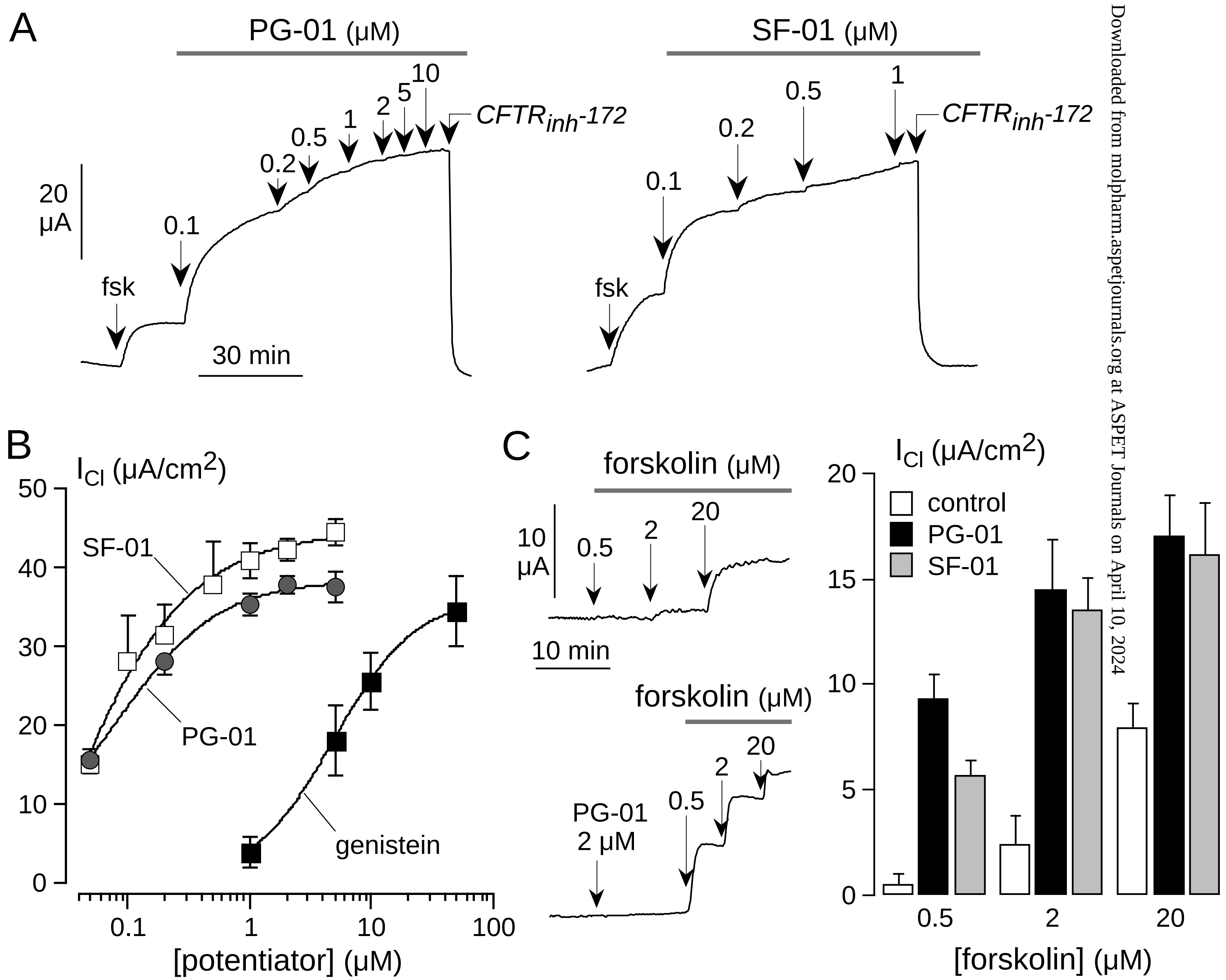

A
PG-01 (μM)
0.1
0.2
0.5
1
2
5
10
CFTRinh-172
20 μA
fsk
30 min
SF-01 (μM)
0.1
0.2
0.5
1
CFTRinh-172
fsk
B
ICl (μA/cm2)
50
40
30
20
10
0
SF-01
PG-01
genistein
0.1
1
10
100
[potentiator] (μM)
C
forskolin (μM)
10 μA
0.5
2
20
10 min
forskolin (μM)
PG-01 2 μM
0.5
2
20
ICl (μA/cm2)
control
PG-01
SF-01
20
15
10
5
0
0.5
2
20
[forskolin] (μM)

Figure 3

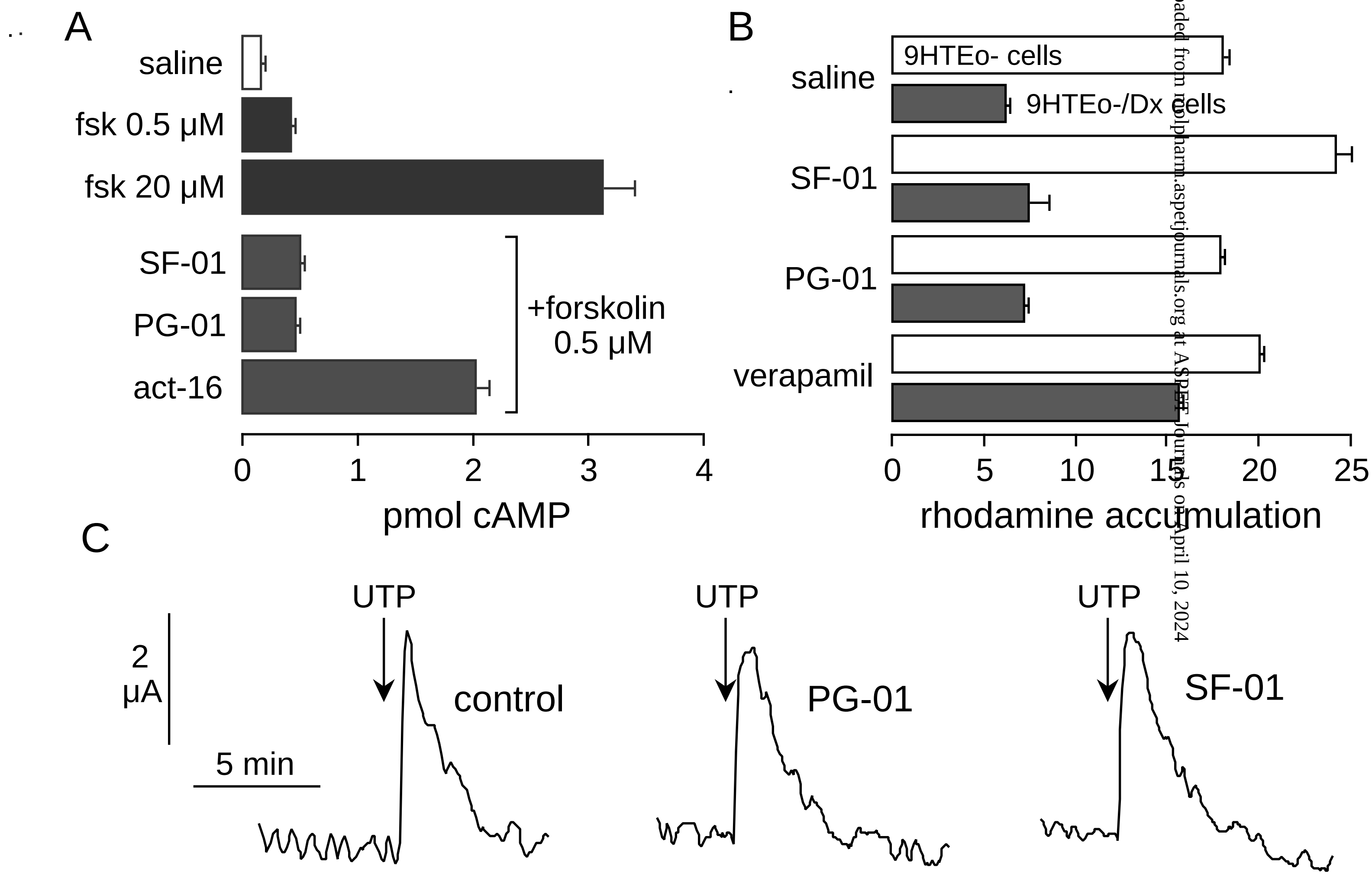
A
saline
fsk 0.5 µM
fsk 20 µM
SF-01
PG-01
act-16
+forskolin
0.5 µM
0
1
2
3
4
pmol cAMP
B
saline
SF-01
PG-01
verapamil
9HTEo- cells
9HTEo-/Dx cells
0
5
10
15
20
25
rhodamine accumulation
C
2
µA
5 min
UTP
control
UTP
PG-01
UTP
SF-01

Figure 4

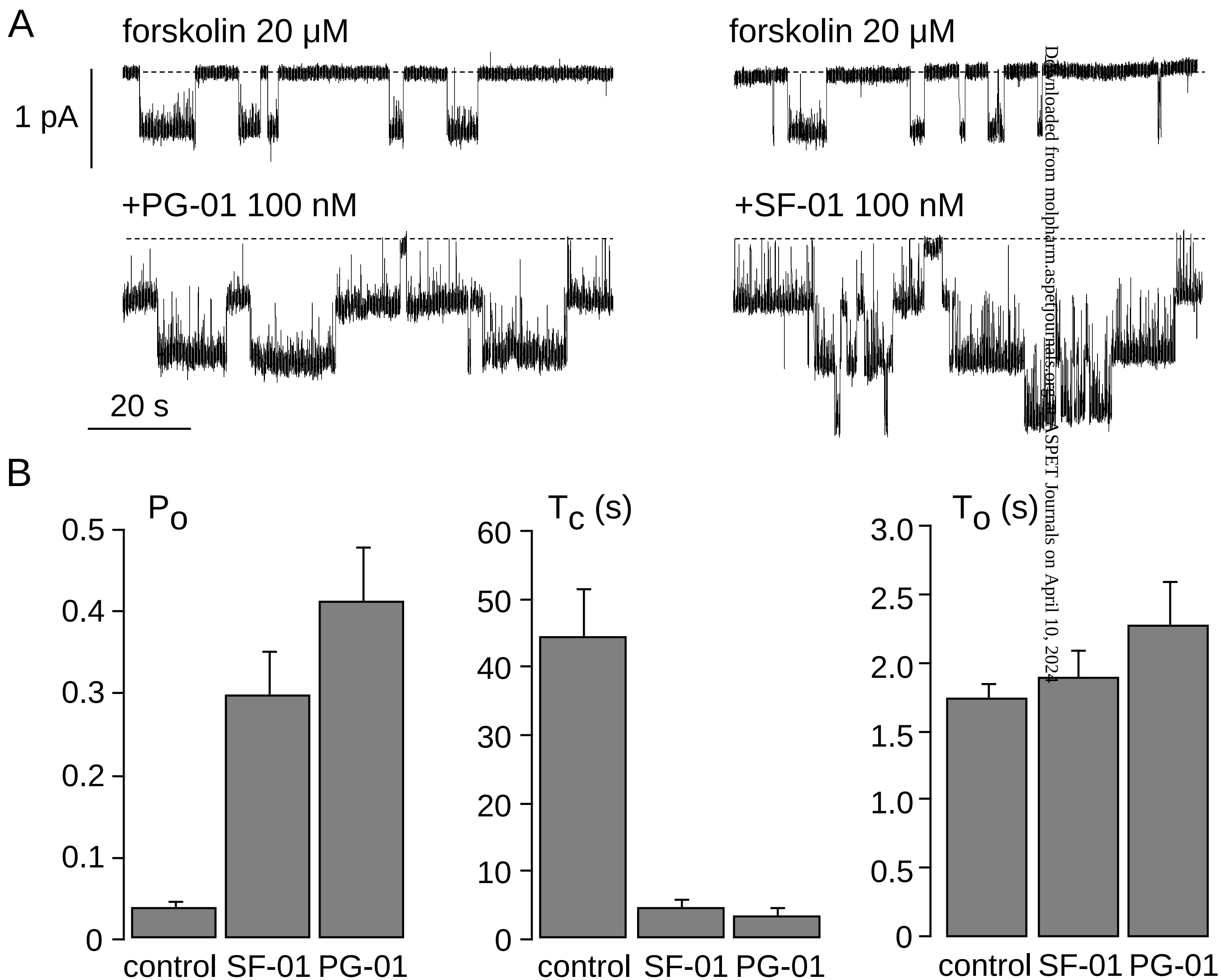
A
forskolin 20 µM
1 pA
+PG-01 100 nM
20 s
forskolin 20 µM
+SF-01 100 nM
B
Po
0.5
0.4
0.3
0.2
0.1
0
control
SF-01
PG-01
Tc (s)
60
50
40
30
20
10
0
control
SF-01
PG-01
To (s)
3.0
2.5
2.0
1.5
1.0
0.5
0
control
SF-01
PG-01

Figure 5

Molecular Pharmacology Fast Forward. Published on February 18, 2005 as DOI: 10.1124/mol.105.010959
This article has not been copyedited and formatted. The final version may differ from this version.

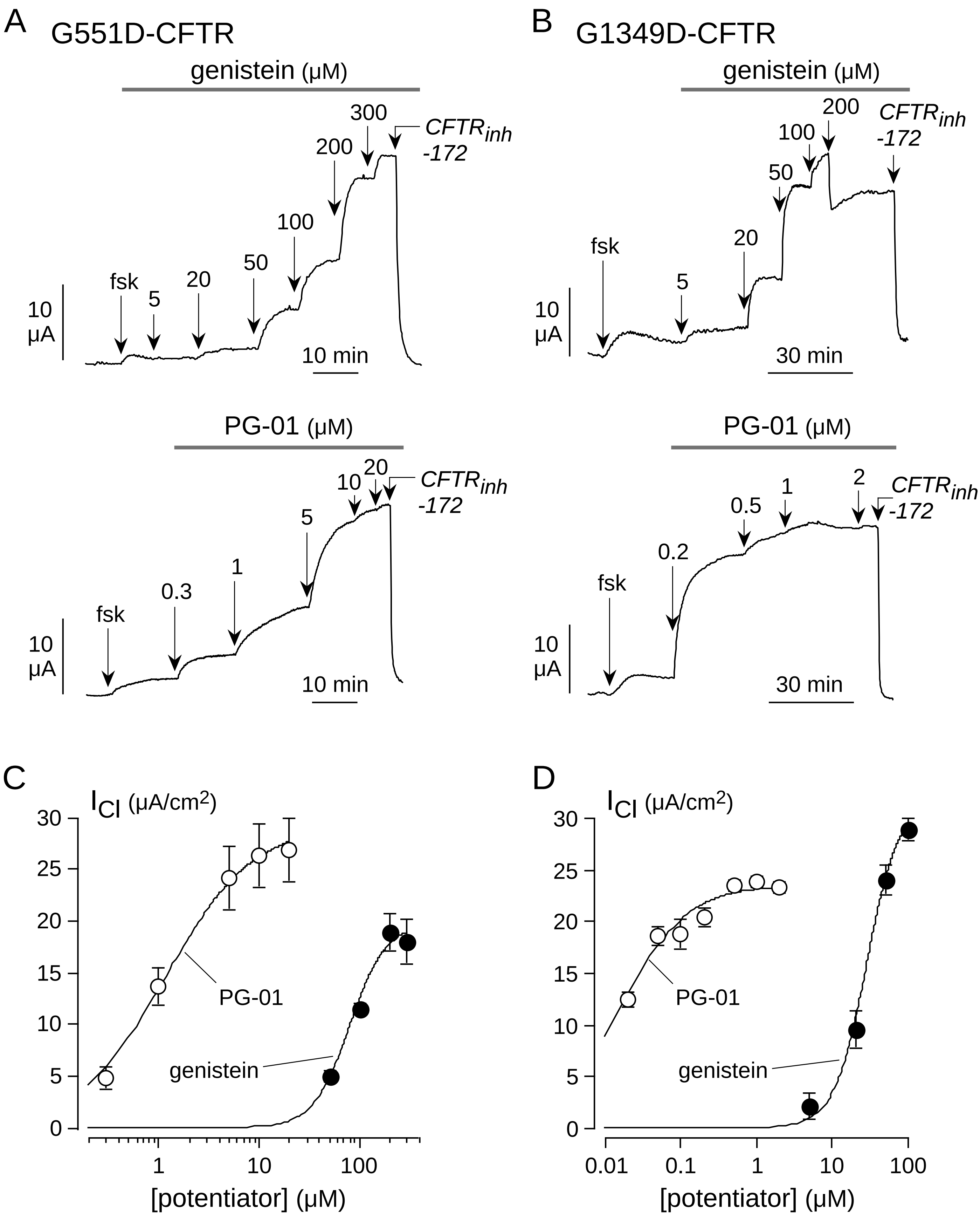

Figure 6

Molecular Pharmacology Fast Forward. Published on February 18, 2005 as DOI: 10.1124/mol.105.010959
This article has not been copyedited and formatted. The final version may differ from this version.

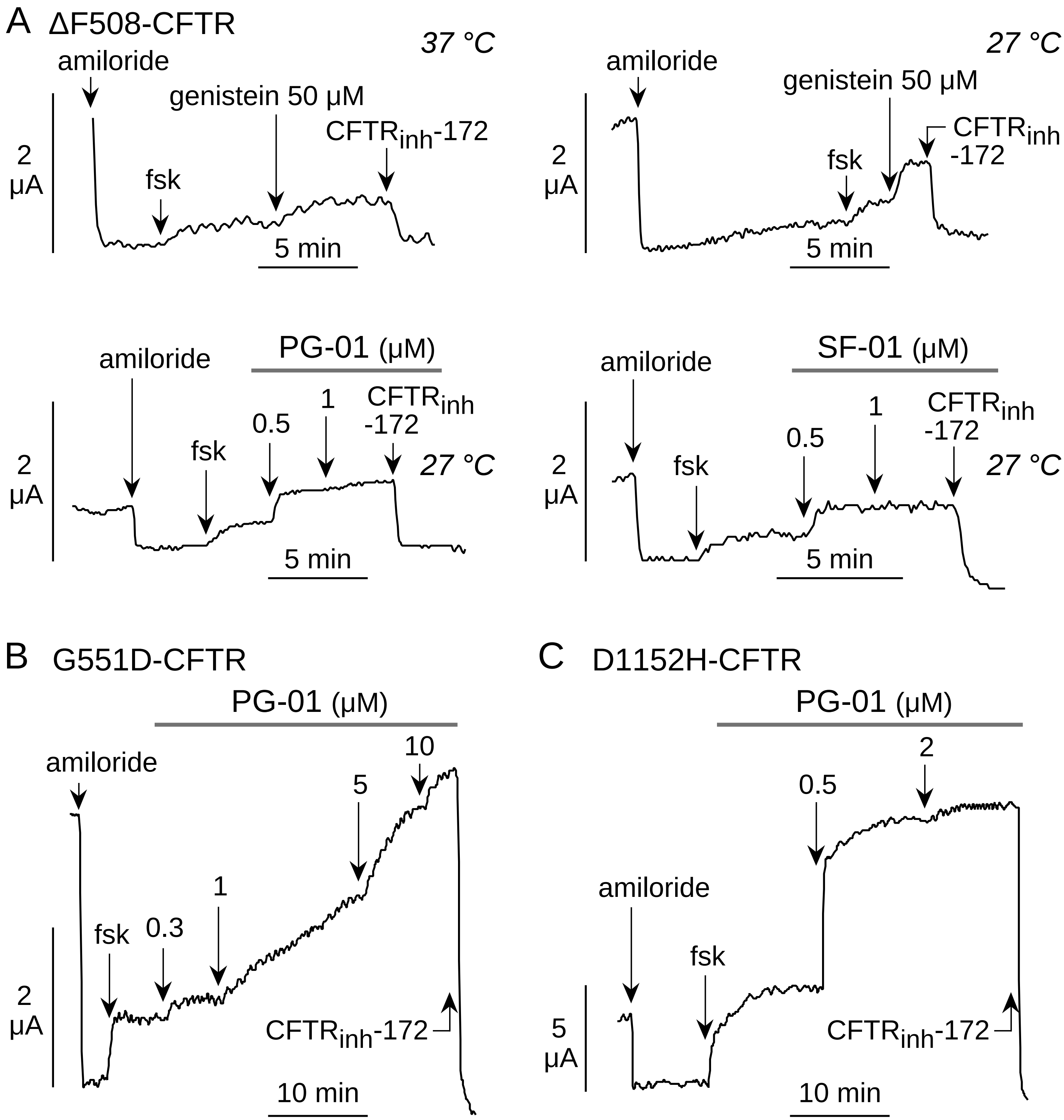

Figure 7

Molecular Pharmacology Fast Forward. Published on February 18, 2005 as DOI: 10.1124/mol.105.010959
This article has not been copyedited and formatted. The final version may differ from this version.

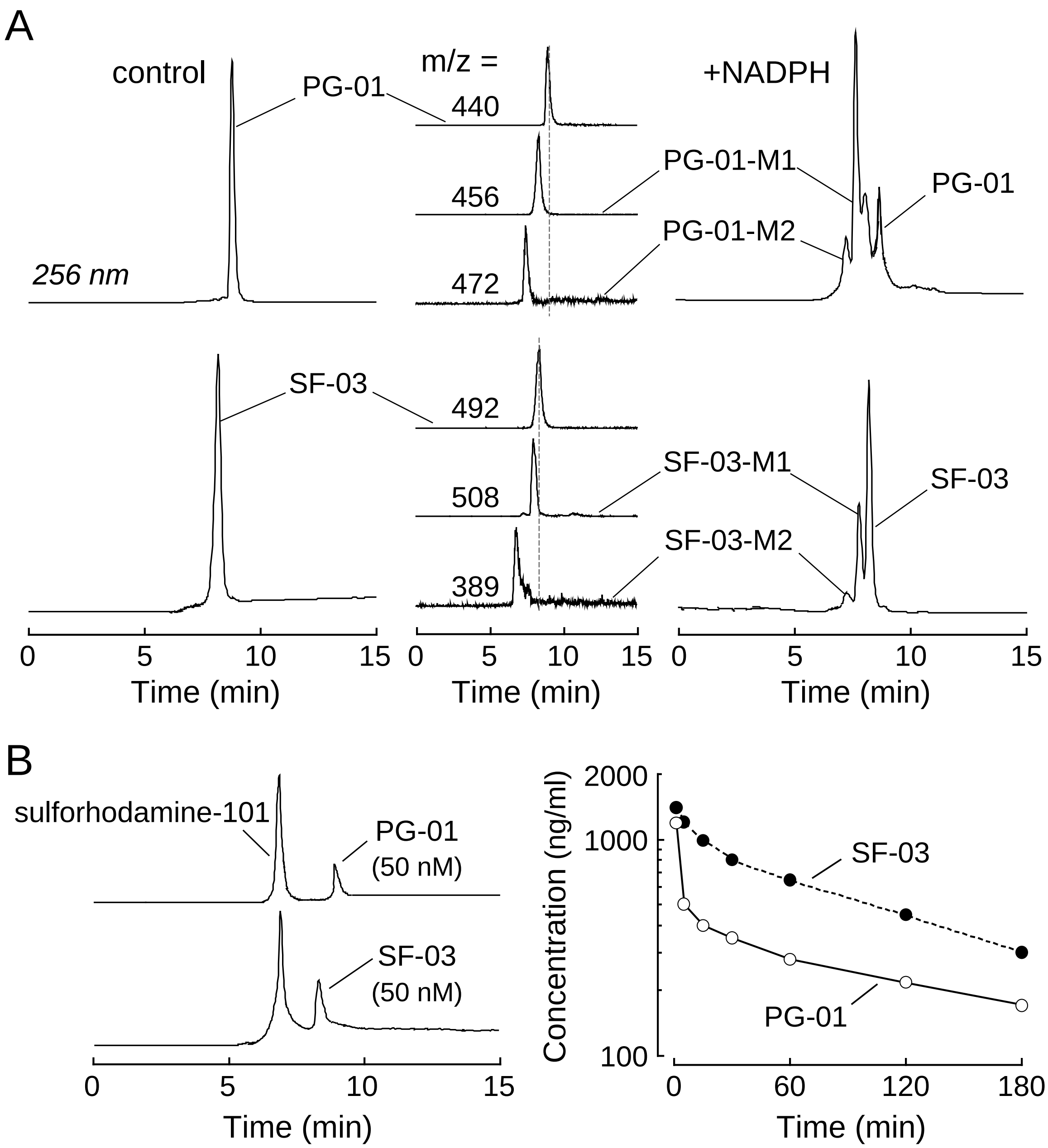

Figure 8